Statistical description of the electronic-level structure of small metallic particles

J. P. Bucher, P. Xia, and L. A. Bloomfield
Department of Physics, University of Virginia, Charlottesville, Virginia 22901
(Received 6 April 1990)

In small metallic particles, the finiteness of the system leads both to a discrete spectrum of the electronic energy levels and to a surface effect due to the boundary conditions. Both effects contribute to the electronic properties of the particles. We analyze the effect of geometry on the energy-level distribution of fcc-type particles, and we discuss the respective roles of the surface irregularities and the underlying crystalline structure. The level-spacing distribution around the Fermi energy is well approximated by a Wigner-Dyson distribution as long as E_F lies in a region of the conduction band where surface-state contributions are dominant. On the band edges, where bulk contributions dominate, remarkable structures may appear in the level statistics that can no longer be approximated by a well-known distribution. We discuss the implications of our results in the general context of finite disordered systems.

I. INTRODUCTION

The concept of level statistics has been widely used to describe the energy-level distribution in small metallic particles, in close analogy with ordinary statistical mechanics. It is assumed that in a real particle, the interactions of an electron are so complicated that the single terms of a Hamiltonian of the system cannot be enumerated and it has been suggested that random matrix theory should be applicable (for a review see Ref. 1). The mean level spacing δ between adjacent one electron levels is given roughly by E_F/N; where N is the number of conduction electrons in the particle and E_F the Fermi energy of the bulk measured from the bottom of the conduction band. In these theories, one considers an ensemble of particles with the same N, but the set of one-electron energy eigenvalues $\{E_n\}$ is supposed to vary from one particle to another (mainly due to differences in surface irregularities of particles pertaining to the same ensemble), and the set of levels is considered as a statistical object defined by the statistical ensemble. The level-spacing distribution is supposed to be well approximated by the Wigner surmise

$$P(\Delta)=C\Delta^n\exp[-\alpha(\Delta/\delta)^2]\ , \tag{1}$$

where $n=1,2\ldots$ depends on particular symmetries of the Hamiltonian and C and α are constants.

The concept of energy-level statistics based on an ensemble of systems has been applied to the description of thermodynamic properties of small particles in the domain $kT<\delta$ where quantum-size effects (QSE) are expected.[2] In this regime only very few levels, 2 or 3, above the ground state of a particle are occupied. The canonical partition function then depends critically on the position of a few individual levels around E_F and so do the physical properties deduced from it. The random matrix theories have been widely used in the interpretation of results from magnetic experiments, particularly the spin susceptibility obtained from conduction-electron spin resonance.[3] It is expected that spin susceptibility should depend strongly on the parity of the number of "conduction" electrons in the particle. Unfortunately, the validity of statistical models has not been demonstrated definitively. Experimentally, several attempts to measure the zero-spin susceptibility of even particles (containing an even number of electrons) at low temperatures have lead to many contradictory results. As evidence for this controversy compare, for instance, measurements of Refs. 4 and 5. Similarly, the validity of random matrix theories has been taken for granted in most speculative works about ac conductivity of small metallic particles.[6] However, no clear, coherent, reproducible experimental results confirm the prediction of these theories. It is true that sample preparation is delicate and the ensemble average is still obscured by a size distribution, which has to be taken into account. In this respect, more recent techniques where mass-selected clusters can be obtained in a rare-gas matrix seem very promising to overcome this difficulty.[7]

Our purpose in this work is to test the applicability of random matrix theories to model the level distribution of a collection of small particles. Since a substantial number of different geometries have to be considered for each ensemble (particles with the same N), we focused on level statistics (calculated from real structures) that are accessible with reasonable computational time. In our calculation we use a tight-binding model with atomic orbitals located on discrete fcc lattice sites. The advantage of using a tight-binding model is that the Hamiltonian matrix contains by construction all the geometrical information of the system. Despite its simplicity and its empirical origin, this model (in connection with graph theory) has been applied successfully to predict the binding energies and ionization potential of alkali-metal clusters of up to ten atoms, in good agreement with *ab initio* calculations.[8] Since the resulting Hamiltonian has time-reversal symmetry and its matrix elements are real, it should be consistent with the statistical orthogonal ensemble ($n=1$) in Eq. (1).

In the past, some attempts have been made to calculate the level statistics by means of simple models: free electrons confined in a plate[9] and in a sphere.[10] However, it is well known that these models show highly degenerated levels which lead to Poisson statistics of the level distribution. For the case of the sphere, each level E_{nl} is $2(2l+1)$ times degenerated. Degeneracy is always connected with symmetry, and since real particles always possess some roughness, the validity of the spherical models is limited to the domain $\Lambda_{nl} < kT < (\Delta E)_{nl}$, where Λ_{nl} is the spread in energy of the originally nondegenerated energy levels and $(\Delta E)_{nl}$ is the average difference between adjacent E_{nl}.[11] Surface irregularities, which play an important role in statistical theories, have been introduced in a perturbative way for the spherical model.[10] But again, the validity of the model is limited to small deformations around equilibrium.

In practice, when we create roughness we must consider discrete lattice sites (with steps and kinks). A real structure with irregularities seems to behave more like a crystal than a liquid drop dominated by surface tension (although surface reconstruction can be considered). This in turn implies that there is an underlying crystalline structure which again possesses some degree of symmetry.

Only recently have the discrete lattice sites been taken into account in statistical calculations by means of a two-dimensional triangular grid,[12] where a surface irregularity parameter proportional to the perimeter of the two-dimensional figure has been defined. Many levels inside a broad window in the middle of the band have been considered. The main result is a bell-shaped level distribution which is progressively better approximated by a Wigner distribution as the roughness of the particles increases.

The purpose of the present work is to extend the calculation to a more realistic three-dimensional fcc structure. In our cluster geometry generation, we take into account the most recent discoveries by transmission electron microscopy (TEM). We consider a more selective range of energy levels around the reference energy E_F than did the authors of Ref. 12. This allows a more careful insight to the respective role of "bulk" and "surface" atoms. We also propose a way to separate the influence of the underlying electronic structure and the surface roughness.

II. MODEL

Without invoking any crystalline structure, it is sufficient for the moment to define a particle as being made of atoms localized on different sites that share at least one coordination (or bond) with each other. Then, for each particle of an ensemble, we consider a one-electron tight-binding Hamiltonian

$$H = T + \sum_{i=1}^{N} V(\mathbf{r} - \mathbf{R}_i) , \tag{2}$$

where V_i is the atomic potential centered at site i of the lattice. We solve the Schrödinger equation by writing each eigenvector ψ_n as a linear combination of atomic orbitals $|i\rangle$ centered on site $\mathbf{R}_i$, assuming one atomic orbital per atom,

$$\psi_n = \sum_i a_i(E_n)|i\rangle . \tag{3}$$

In addition, we neglect overlap integrals of functions centered on different sites so that

$$\langle i|j\rangle = \delta_{ij} . \tag{4}$$

By introducing the implicit statement that $|i\rangle$ must be an atomic eigenstate with eigenvalue E_0^i, and by neglecting the integrals of the type $\langle k|V_j|i\rangle$ that involve three functions centered on different sites, since those functions are very localized, we can write the Schrödinger equation as

$$(E_0^k - E_n + \alpha_k)a_k + \sum_{i \neq k} \beta_{ki} a_i = 0 , \tag{5}$$

where

$$\beta_{ki} = \langle k|V_k|i\rangle \tag{6}$$

are the two-center hopping integrals, and

$$\alpha_k = \left\langle k \left| \sum_{j \neq k} V_j \right| k \right\rangle \tag{7}$$

are the crystal-field integrals. The β's represent the coupling between atoms. In a perturbational sense, they produce the splitting of the energy levels and determine the bandwidth. On the other hand, the α's express the perturbation of the atomic potential by the crystal field and they determine the shift of the band. For simplicity and without loss of generality, we put

$$E_0^k + \alpha_k = 0 . \tag{8}$$

In compact structures such as fcc, it is usual to take nonzero β's only between nearest-neighbor (NN) atoms,

$$\beta_{ij} = \begin{cases} -1 & \text{if } i \text{ and } j \text{ are NN} \\ 0 & \text{otherwise} . \end{cases} \tag{9}$$

For a given structure (fcc) this defines the matrix of the β's, which contains nothing but the information of the geometry of the particle. It is equivalent to an incidence matrix used in electrical network analysis. The energy scaling for the β's defined in Eq. (9) is convenient since the coordination number or number of NN for site i is given by

$$z_i = \sum_{j=1}^{N} |\beta_{ij}| . \tag{10}$$

The total coordination number of the whole particle is

$$Z = \sum_{i=1}^{N} z_i , \tag{11}$$

where $z_i \leq 12$ for a fcc lattice.

By solving Eq. (5), we obtain the sets of eigenvalues $\{E_n\}$ and eigenstates $\{a_i(E_n)\}$ of the Hamiltonian and the density of states (DOS) is given by

$$n(E) = (1/N) \sum_{n=1}^{N} \delta(E - E_n) . \tag{12}$$

The local density of states (LDOS) on site i is given by

$$n_i(E)=\sum_{n=1}^{N}|a_i(E_n)|^2\delta(E-E_n)\ . \tag{13}$$

For properties like electronic specific heat and magnetic susceptibility, we are only interested in the level distribution within a few kT from the highest occupied level at $T=0$, the Fermi level E_F, defined by

$$\int_{-\infty}^{E_F} n(E)dE=Q\ , \tag{14}$$

where Q is the band filling, equal to $\frac{1}{2}$ in the case of one s electron per atom.

It is sometimes useful to define the pth moment of the DOS

$$\mu_p=\int_{-\infty}^{+\infty}E^p n(E)dE=\frac{1}{N}\mathrm{Tr}(H^p)\ . \tag{15}$$

The first moments μ_1, μ_2, and μ_3 are then related, respectively, to the shift of the band, the bandwidth, and the asymmetry of the band. In our tight-binding framework

$$\mu_2=\beta^2(Z/N)\ . \tag{16}$$

The procedure we employ consists of solving Eq. (5) for each particle m of the ensemble. For each set $\{E_n\}_m$, only a few levels around the reference energy (i.e., E_F) are considered as contributing to the level statistics.

III. GEOMETRY GENERATION AND CALCULATION

In this section we discuss the technique used to generate an ensemble of particles having the same number of atoms N but with different shapes. Once each particle geometry has been determined, its Hamiltonian matrix can be diagonalized and the level-spacing statistics can be recorded. This procedure is repeated many times to ob-

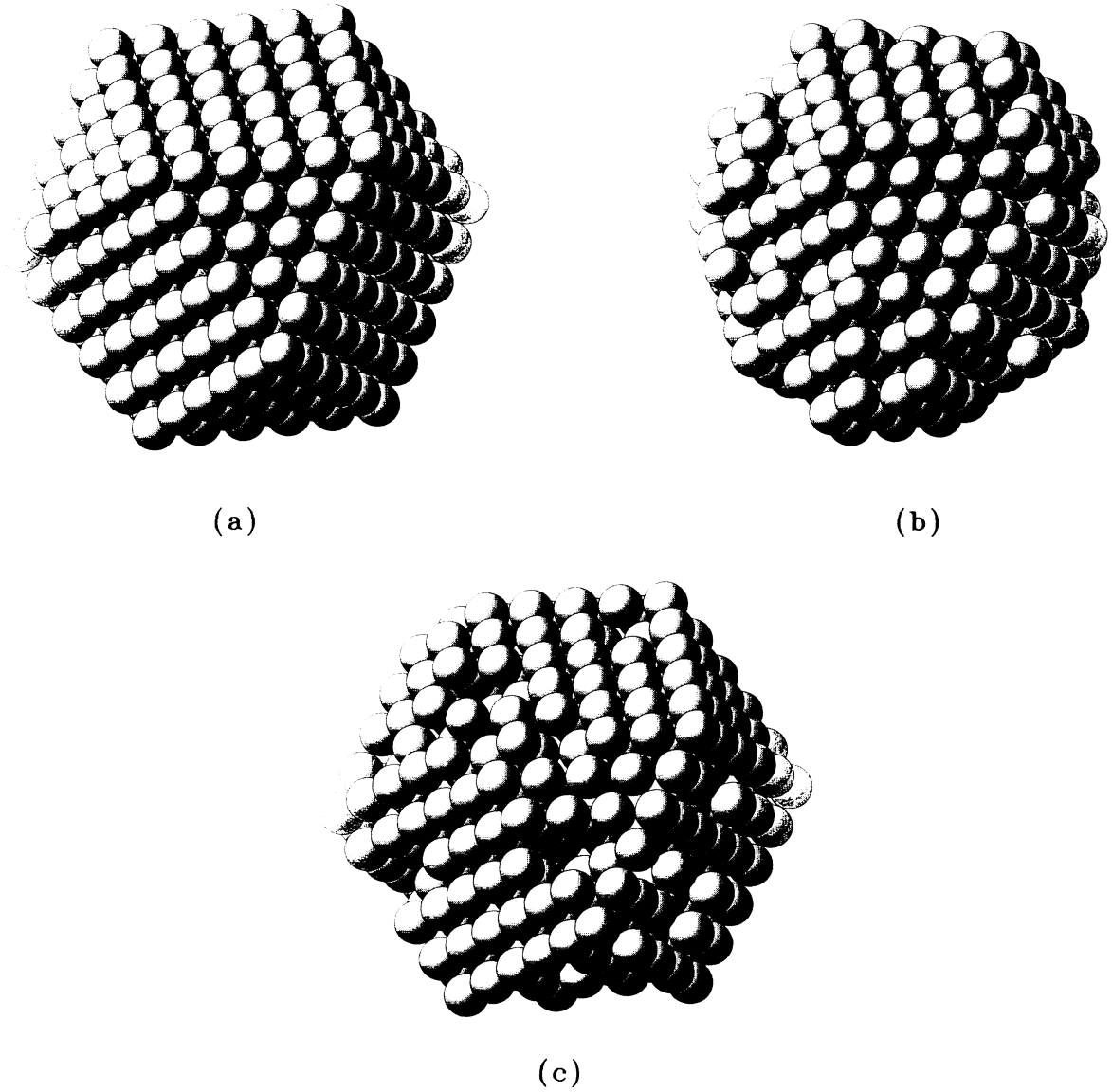

FIG. 1. Geometrical structures for (a) a filled-shell cubooctahedron of 561 atoms; (b) and (c) Particles of 454 atoms obtained by geometrical generation with $\rho=1.04$ and 1.83, respectively.

tain the relevant statistics for the ensemble.

Recent TEM experiments on metal particles deposited on various insulating films show that the gross geometries of such particles are well defined. Although the equilibrium geometries are affected by the nature of the support and the preparation technique, the general trend is that particles that normally crystallize in the fcc structure show a fivefold symmetry (icosahedrons) for small sizes, while for bigger sizes the most frequently observed structure is an fcc cubooctahedron. These results are confirmed by recent electron-diffraction experiments on unsupported Ag particles in a molecular beam: for particles of about 2 nm in diameter, icosahedral and fcc-cubooctahedral structures coexist in the beam, while for bigger sizes only the well-defined fcc structure is observed.[13] The icosahedral structures can be obtained from the cubooctahedral ones by a slight distortion that minimizes the surface energy for small clusters, as shown by Ino.[14] Some metals, like Pt, keep their fcc structures down to very small sizes (1.5 nm).[15,16] Others, like Au, show an icosahedral structure up to a few nm,[17] although small Au cubooctahedral particles have also been observed.[18,19]

In our calculations, we consider particles big enough that we treat only the cubooctahedral case. Therefore we assume that only sites on an fcc lattice are permitted. The cubooctahedron [see Fig. 1(a)], like its icosahedral counterpart, can be constructed layer by layer around a central atom (see Table I). The first cubooctahedron has 13 atoms ($m=2$), the second 55 ($m=3$), the third 147 ($m=4$), etc.

However, it is highly improbable that a collection of particles would be made up only of filled-shell cubooctahedra. In TEM data, particles with unfilled shells are clearly shown; some of them possess missing edge atoms.[18,20] In order to account for incomplete shells and surface roughness, we simulate the real geometry in the following way. We start with a filled-shell cubooctahedron, heat it up, and allow the atoms to desorb according to the probability proportional to

$$\exp(-E_B^i/kT) , \tag{17}$$

where E_B^i is the binding energy of the atom under consideration on site i. This procedure is repeated until we get the right number of atoms N in the particle. E_B^i is given by

$$E_B^i = -\int_{-\infty}^{E_F} E\, n(E) dE . \tag{18}$$

For a nearly half-filled band, it is easy to show that

$$E_B^i = a(Q)|\beta| z_i^{1/2} , \tag{19}$$

consistent with our tight-binding model. $a(Q)$ is a parameter which depends only on the band filling Q.

Since the matrix of the β's contains all the information about the geometry, it is useful to update this matrix at each desorption step and register the number of broken bonds [i.e., the coordination number of the atom which has been removed according to Eq. (10)]. When removing one atom on site i, the new Hamiltonian matrix is obtained from the old one by removing line i and column i in the matrix of the β's. To obtain the actual coordination number Z of the particle, we must subtract the total amount of broken bonds from the total coordination number Z_0 of the complete cubooctahedron (Table I).

It is convenient to define a roughness parameter ρ which facilitates the comparison between particles of different sizes but similar surface irregularities

$$\rho = \frac{1}{36}\left[\frac{10}{3}\right]^{2/3} \frac{1}{N^{2/3}}(Nz_b - Z) . \tag{20}$$

For a given N, it is proportional to the surface exposed, or to the total number of noncoordinated surface bonds ($Nz_b - Z$), where $z_b = 12$ is the coordination number of a fcc bulk atom and Z is the total coordination number of the particles given by Eq. (11). The $N^{2/3}$ term refers to an ideal surface. The numerical factor is chosen so that $\rho = 1$ for an infinitely big cubooctahedron, limited only by (111) and (100) planes with atomic coordination of 9 and 8, respectively. The number of atoms of a given type in a perfect cubooctahedron are given in Table I.

TABLE I. List of the number of atoms of a given type in a regular cubooctahedron; m is the shell number, $m \geq 2$; $m=2$ corresponds to the first 13 atoms cubooctahedron.

Total	$\frac{10}{3}m^3 - 5m^2 + \frac{11}{3}m - 1$
Surface	$10m^2 - 20m + 12$
Corner	12
Edge	$24(m-2)$
(111) face	$4(m-2)(m-3)$
(100) face	$6(m-2)^2$
Total coordination number	$Z_0 = 40m^3 - 96m^2 + 80m - 24$

IV. RESULTS AND DISCUSSION

Calculations have been done for four different ensembles. Each ensemble is characterized by the number N of atoms contained in its particles and its average value of ρ (the roughness). For each size, $N=88$ and $N=454$, two values of the parameter ρ have been considered. The calculation involves 4000 particles for the $N=88$ ensembles and 600 particles for the $N=454$ ensembles. Typical coordination number distributions for particles obtained by geometry generation with $N=454$ are shown in Fig. 2. For each particle, the precursor geometry was a cubooctahedron of 561 atoms. Particles representative of these ensembles are shown in Figs. 1(b) and 1(c). Interestingly enough, Fig. 1(b) reproduces well the TEM result that particles of this size possess missing corner and edge atoms (less coordinated).[18,20] For comparison, Fig. 1(c) shows a particle with a much higher surface roughness. Those particles have holes and protruding atoms. They do not match TEM observations but show an interesting limiting case.

Unless specified, we consider half-filled bands and we focus on level statistics of a few levels around the Fermi

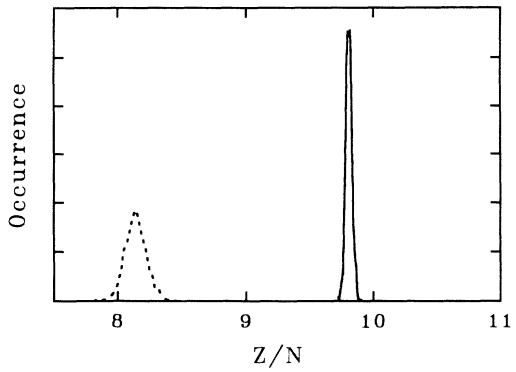

FIG. 2. Coordination number distributions for particles of 454 atoms. Two ensembles of 600 particles leading to two different average roughnesses $\rho=1.04$ (solid line) and $\rho=1.83$ (dashed line) have been considered. Typical particles of these ensembles are shown in Figs. 1(b) and 1(c).

energy: 8 for $N=88$ and 40 for $N=454$. Figures 3 and 4 show the corresponding level-spacing statistics for two different values of ρ. The best fit is obtained with a Wigner distribution by putting $n=1$ in Eq. (1). A remarkable fact is that the maximum of the distribution shifts towards smaller Δ's as the roughness increases. The effect seems to be more important for smaller particles. As we explain later, it is related to the fact that the relevant parameter for the average level spacing is not ρ but $Z^{1/2}/N^{3/2}$. The average level spacing δ is given in the figure captions and is not constant for a given N. Such an effect has not been mentioned by the authors of Ref. 12 for the two-dimensional case.

Despite the effects mentioned above, near the middle of the band there is no drastic difference in the features of the statistics for different ensembles. This can best be seen by changing the argument in Eq. (1) to $x=\Delta/\delta$. In this representation, and within the precision of our calcu-

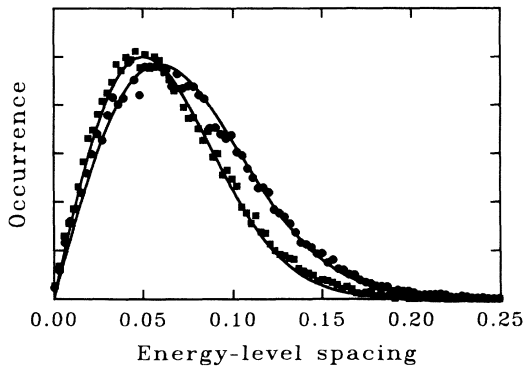

FIG. 3. Level-spacing distributions for particles of 88 atoms. Two ensembles of 4000 particles have been considered. For each particle, the calculation involves the eight first levels around $E_F=0$. We also give the respective values δ^2/α of the fit with a Wigner distribution of Eq. (1). ●, $\rho=1.00$, $\delta^2/\alpha=7\times10^{-3}$; ■, $\rho=1.83$, $\delta^2/\alpha=5\times10^{-3}$. The energy scale is in β units.

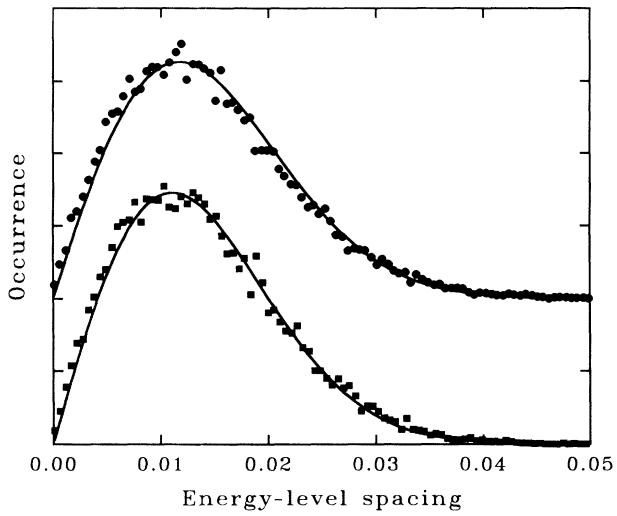

FIG. 4. Level-spacing distributions for particles of 454 atoms. Two ensembles of 600 particles have been considered. For each particle, the calculation involves the 40 first levels around $E_f=0$. ●, $\rho=1.04$, $\delta^2/\alpha=2.75\times10^{-4}$; ■, $\rho=1.83$, $\delta^2/\alpha=2.45\times10^{-4}$. The energy scale is in β units.

lations, all the statistics of Figs. 3 and 4 look the same and can be fitted by $P(x)=(\pi/2)x\exp(-\pi x^2/4)$. It is not possible to distinguish this distribution from the more general Brody distribution [Eq. (5.30) of Ref. 1] where the parameter ω must be equal to 1 to fit our data properly.

On the other hand, level distributions in Fig. 5 ($N=454$; $\rho=1.04$), calculated at the bottom and top of the band, show completely different features and reflect some more fundamental structures. The top of the band, Fig. 5(b) shows a nonzero contribution for $\Delta=0$ and is much closer to a Poisson distribution. We find that the average level spacing δ varies over the band. For the ensemble ($N=454$, $\rho=1.04$) and assuming $\alpha=\pi/4$ in Eq. (1), as appropriate for the orthogonal ensemble,[2] we find $\delta=1.47\times10^{-2}$ in the middle of the band, but $\delta=0.9\times10^{-2}$ for the Poisson distribution at the top of the band. It is not possible to fit the statistics of Fig. 5(a) with any known distributions. This is due to the long tail and to the distinct peak at a level spacing of about 0.9. This peak may be due to localized states since it appears statistically for different boundaries.

In order to understand the features observed in Figs. 3–5, we must address the question of how the geometrical characteristics of the particles like the roughness ρ influence the electronic structure and level distribution at various points in the band. For this purpose, we assume that particles contain sites that contribute to the "bulk" part ($z_i=12$) of the DOS as well as sites that contribute to the "surface" part ($z_i<12$). We define the LDOS according to Eq. (13). Figures 6(a) and 6(b) show the average surface DOS and the average bulk DOS for particles with $N=454$ atoms and two different roughnesses. Figures 6(a) and 6(b) are histograms (averaged over several configurations close to ρ) and do not display the fine structure of the levels which are used in the statistics.

Figure 6 contains part of the answer to our question.

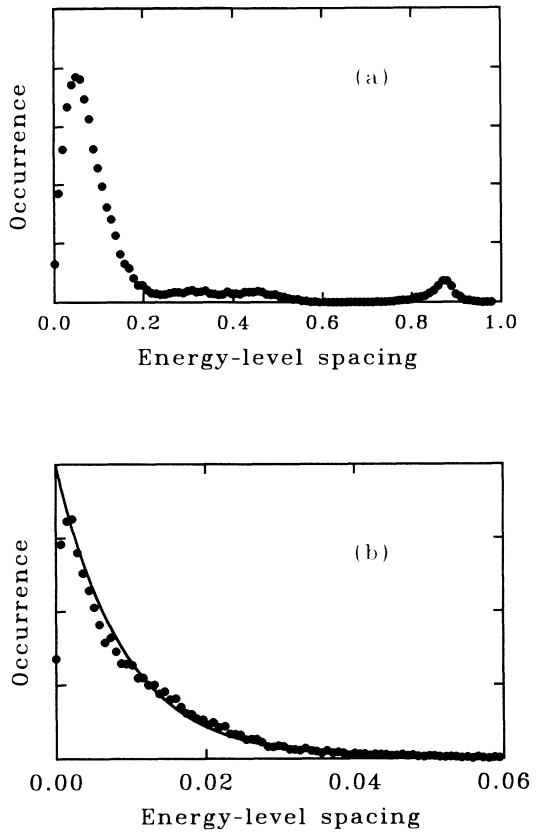

FIG. 5. Level-spacing distributions for particles of 454 atoms with $\rho=1.04$ calculated at (a) the bottom of the band and (b) the top of the band. The solid line shows the best fit to a Poisson distribution: $P(\Delta)=C\exp(-\Delta/\delta)$ with $\delta=9\times10^{-3}$. The ensemble is made of 600 particles and for each particle the first 40 levels from the bottom and the top of the band, respectively, are considered.

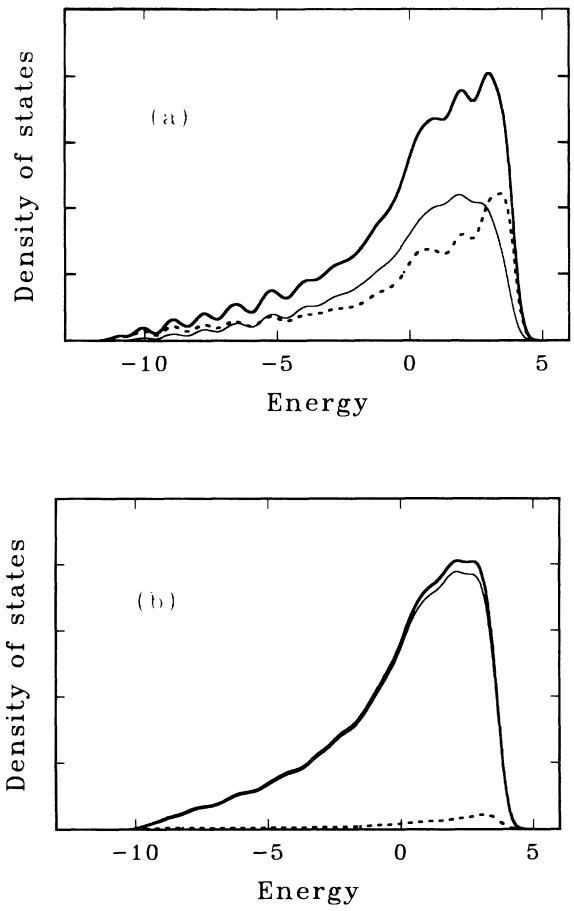

FIG. 6. Total DOS (bold line) as well as bulk (dashed line) and surface (thin line) contribution to the total DOS for the $N=454$ ensemble. (a) $\rho=1.04$, (b) $\rho=1.83$. Each DOS is an average over ten configuration close to the given values of ρ.

For the smooth particles of Fig. 6(a) (the only ones that are observed physically) the surface contribution to the total DOS is dominant in the middle of the band. This behavior is completely reversed at the band edges, where only bulk sites contribute to the total DOS. Consequently, the unusual level-spacing distribution at the band edges (Fig. 5), in particular the spectral rigidity observed at the band bottom, seems to be due mainly to bulk states. As the roughness increases [Fig. 6(b)], the LDOS of bulk atoms follows more closely the trend of the surface LDOS. The features that we obtain for the band bottom look very different from the peaked statistics without any structure that is obtained in the two-dimensional case by Tanaka and Sugano.[12] Rather than an effect of dimensionality, we believe that the very sharp statistics of their Fig. 8 could be due to their consideration of only one level spacing at the very band bottom in conjunction with their somewhat unusual definition of x, the argument of the distribution. It is questionable to which extent Fig. 8 of Ref. 12 can be considered as a level-spacing statistics since only one level above E_F is taken into account.

Also evident from our Figs. 6(a) and 6(b) is that creating roughness causes the bandwidth to become narrower. The explanation of this behavior is straightforward if we notice that poorly coordinated atoms retain their atomic character and therefore contribute essentially to states around $E=0$. This has an important effect on the level statistics. We can discuss this in a more quantitative way. The bandwidth is proportional to $\mu_2^{1/2}$ and thus to $Z^{1/2}$ [Eq. (16)]. As a consequence, the energy levels become more dense in the middle of the band as Z decreases (increasing roughness). Since surface roughness ensures a complete lifting of the degeneracies in the middle of the band, the actual level spacing varies as $Z^{1/2}/N^{3/2}$, on the average. This explains the behavior observed in Figs. 3 and 4 where the maximum of the distribution shifts towards lower values of the level spacing as the roughness increases.

The main result of this study shows that, especially in the domain of moderated surface irregularities as they are encountered in TEM, the applicability of the random matrix theories depends very much on the band filling or on the position of E_F in the conduction band. The Wigner

distribution is applicable for a half-filled band (typical of Na) while the Poisson distribution is more appropriate for a nearly filled band (typical of Mg).

It must be stressed that our description of surface irregularities only leads to a restricted notion of disorder. Since the metallic particles under consideration here are supposed to be crystalline we did not explicitly introduce diagonal disorder in our Hamiltonian. The implications of a finite disordered system have been analyzed numerically within the tight-binding framework by Sivan and Imry.[21] In the strong disorder limit, they found a Wigner-type distribution with a relevant parameter δ in Eq. (1) proportional to the hopping integral β rather than to the standard deviation of the diagonal term in the Anderson Hamiltonian. Their result is in fair agreement with analytical results by Efetov.[22] In terms of Anderson's description, our model corresponds to the limit of weak disorder which implies $hD/L^2 \gg \beta(Z/N)^{1/2}$, where D is the diffusion constant and L the characteristic length of the particles.

In this work we have focused on level calculations *per se*, but physical properties like the spin susceptibility can also be obtained from the energy-level distribution in a straightforward manner.[11] In concluding, we wish to remark that difficulties of extracting informations from experimental data to compare to theoretical level distribution is considerable. Susceptibility measurements give an indirect access to the level distribution around E_F. In fact, it provides a measure of the average level spacing inside a window approximately defined by the width of the distribution $\partial f(E,T)/\partial E$ (a few kT); where f is the Fermi function. If for some reason the electronic Zeeman energy in the external magnetic field is bigger than δ or if the levels are smeared out, i.e., by the interaction with thermal phonons, the susceptibility measurement will not reflect the calculated level spacing. As far as QSE are concerned, it has been emphasized recently[23] that due to the clear signature of the Korringa relaxation mechanism, the evidence for QSE could be tested by NMR at any temperature without reference to any type of ensemble.

ACKNOWLEDGMENTS

The authors gratefully acknowledge support of the Office of Naval Research, Grant No. 00014-88-K0422. One of us (J.P.B.) acknowledges support from the Swiss National Science Foundation, Grant No. 8220-025964.

[1]T. A. Brody, J. Flores, J. B. French, P. A. Mello, A. Pandey, and S. S. M. Wong, Rev. Mod. Phys. **53**, 385 (1981).
[2]J. A. A. J. Perenboom, P. Wyder, and F. Meier, Phys. Rep. **78**, 173 (1981); W. P. Halperin, Rev. Mod. Phys. **58**, 533 (1986).
[3]R. Kubo, A. Kawabata, and S. Kobayashi, Ann. Rev. Mater. Sci. **14**, 49 (1984).
[4]K. Kimura and S. Bandow, Phys. Rev. Lett. **58**, 1359 (1987).
[5]S. Pasche and J. P. Borel, Z. Phys. D **12**, 401 (1989).
[6]L. M. Gor'kov and G. M. Eliashberg, Zh. Eksp. Teor. Fiz. **48**, 1407 (1965) [Sov. Phys.—JETP **21**, 940 (1965)]; K. Frahm, B. Muehlschlegel, and R. Nemeth, Z. Phys. B **78**, 91 (1990).
[7]D. M. Lindsay, F. Meyer, and W. Harbich, Z. Phys. D **12**, 15 (1989).
[8]Y. Wang, T. F. George, D. M. Lindsay, and A. C. Beri, J. Chem. Phys. **86**, 3493 (1987), and following article.
[9]J. Barojas, E. Costa, E. Blaisten-Barojas, J. Flores, and P. A. Mello, Ann. Phys. **107**, 95 (1977).
[10]K. F. Ratcliff, in *Multivariate AnalysisV,* edited by P. R. Krishnaiah (North-Holland, Amsterdam, 1980).
[11]J. P. Bucher and J. J. van der Kink, Helv. Phys. Acta **61**, 760 (1988).
[12]S. Tanaka and S. Sugano, Phys. Rev. B **34**, 740 (1986).
[13]B. Hall, M. Flueli, R. Monot, and J. P. Borel, Z. Phys. D **12**, 97 (1989).
[14]S. Ino, J. Phys. Soc. Jpn. **27**, 941 (1969).
[15]M. J. Yacaman, S. Fuentes, and J. M. Dominguez, Surf. Sci. **106**, 472 (1981).
[16]M. L. Sattler and P. N. Ross, Ultramicroscopy **20**, 21 (1986).
[17]M. Flueli, R. Spycher, P. A. Stadelmann, P. A. Buffat, and J. P. Borel, Europhys. Lett. **6**, 349 (1988).
[18]S. Ijima and T. Ichihashi, Phys. Rev. Lett. **56**, 616 (1986).
[19]M. Flueli and J. P. Borel, J. Cryst. Growth **91**, 67 (1988).
[20]O. L. Perez, D. Romeu, and M. J. Yacaman, Appl. Surf. Sci. **13**, 402 (1982).
[21]U. Sivan and Y. Imry, Phys. Rev. B **35**, 6074 (1987).
[22]K. B. Efetov, Adv. Phys. **32**, 53 (1983).
[23]J. J. van der Klink, Z. Phys. D **12**, 15 (1989).

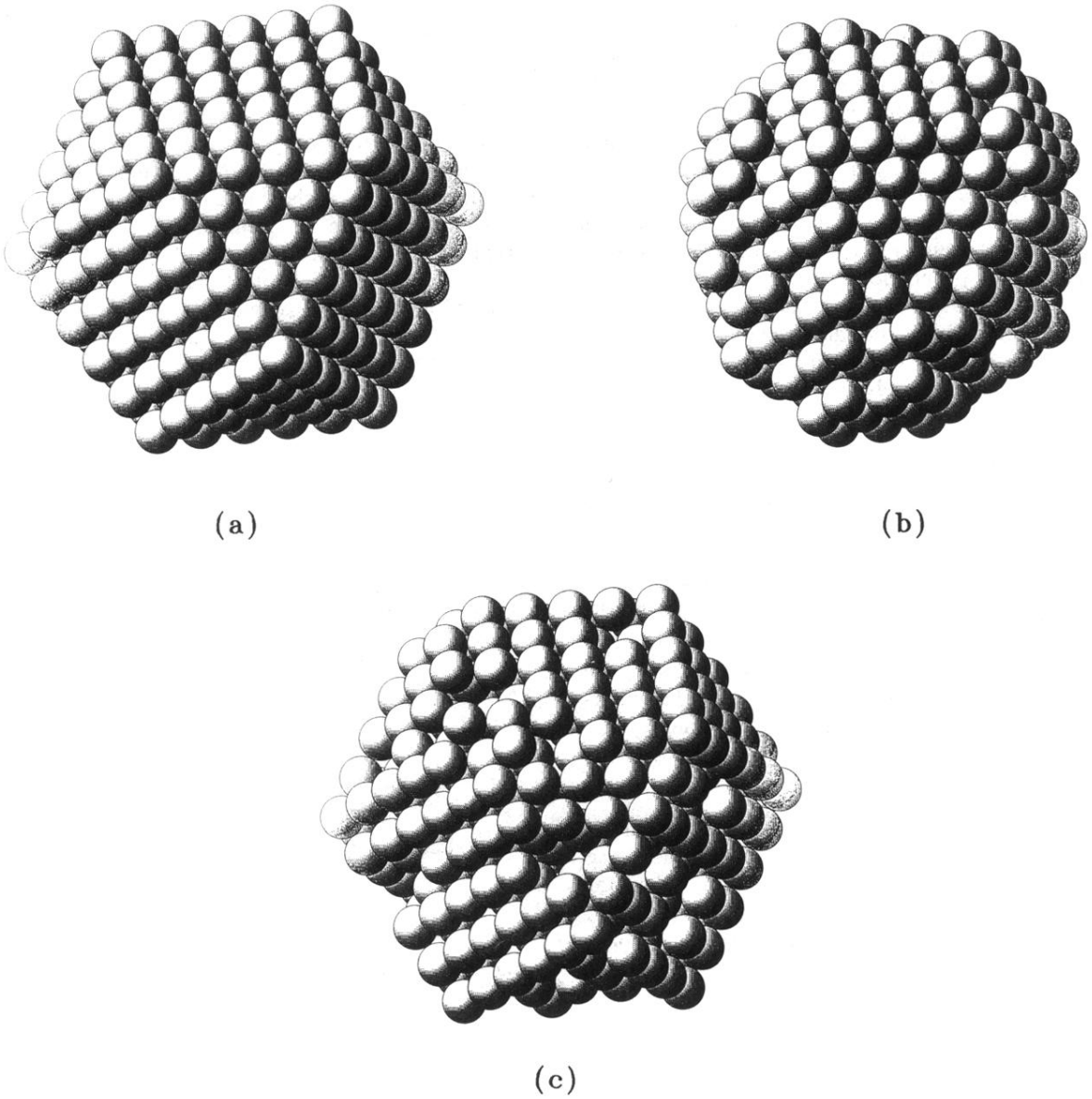

FIG. 1. Geometrical structures for (a) a filled-shell cubooctahedron of 561 atoms; (b) and (c) Particles of 454 atoms obtained by geometrical generation with $\rho = 1.04$ and 1.83, respectively.